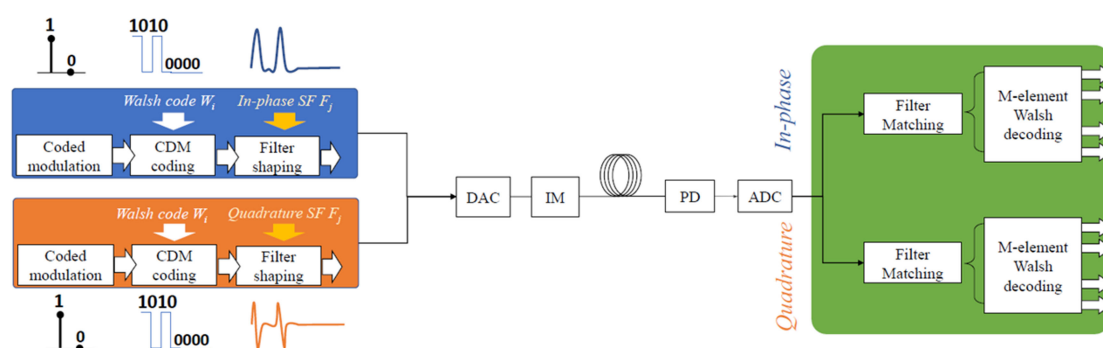


Hybrid Coding and Filtering Technique for Optical IM-DD Link With Robustness to Multipath Interference and Bandwidth Limitation

Volume 13, Number 2, April 2021

Lin Sun
Gai Zhou
Qirui Fan
Alan Pak Tao Lau
Changjian Guo
Chao Lu



DOI: 10.1109/JPHOT.2021.3065025

Hybrid Coding and Filtering Technique for Optical IM-DD Link With Robustness to Multipath Interference and Bandwidth Limitation

Lin Sun , Gai Zhou , Qirui Fan , Alan Pak Tao Lau ,
Changjian Guo , and Chao Lu 

Photonics Research Center, Department of Electrical Engineering, The Hong Kong Polytechnic University, Hung Hom, Kowloon, Hong Kong SAR, China
The Hong Kong Polytechnic University Shenzhen Research Institute, Shenzhen 518057, China

DOI:10.1109/JPHOT.2021.3065025

This work is licensed under a Creative Commons Attribution 4.0 License. For more information, see <https://creativecommons.org/licenses/by/4.0/>

Manuscript received December 18, 2020; revised February 16, 2021; accepted March 7, 2021. Date of publication March 12, 2021; date of current version April 7, 2021. This work was supported by the National Key R&D Program of China Project 2019YFB1803502. Corresponding author: Lin Sun (e-mail: linsanity.sun@polyu.edu.hk).

Abstract: In this work, a hybrid code division multiplexing (CDM) coding and digital filtering method for optical intensity modulation and direct detection (IM-DD) link is investigated to address multipath interference (MPI) and channel bandwidth limitation. CDM signaling already provides robustness to MPI through suppressing the unsynchronized paths by orthogonal (de)coding. As for digital filtering based on square root raised cosine (SRRC) waveforms, its advantage to IM-DD link includes robustness to channel bandwidth limitation due to pulse shaping. Additionally, matching filters achieve the best orthogonality only when they are synchronized well, thus robustness to MPI can be expected on the basis of CDM. We study the performance of such hybrid coding and filtering method over IM-DD link in the presence of MPI and bandwidth limitations through simulation. This is followed by experimental demonstrations of single point-to-point transmission with capacity at 112 Gbps. BER comparison between CDM only and hybrid filtering and coding method is performed by emulating MPI using a Mach-Zehnder interferometer. Furthermore, bidirectional transmission over a single fiber verifies its performance advantage and demonstrates potentials for reducing implementation costs of end-to-end optical communications.

Index Terms: Electro-optical systems, optical interconnects.

1. Introduction

Recent years, optical intensity modulation and direct detection (IM-DD) solution exhibits its advantages in short reach optical communication application, with low power consumption and economical implementation [1]. Comparing with coherent detection technique, rate performance of single point-to-point IM-DD link is more limited by channel bandwidth limitation. That is caused by the limited bandwidth of electrical and optical devices, and fiber dispersion as well [2]. Moreover, IM-DD systems are more sensitive to multipath interference (MPI) caused by optical reflections at discrete points in the link [3]. That is because MPI not only results in the delayed copies of signal but also interferometric noise. Signal degradation due to MPI have been investigated in optical

N-level pulse amplitude modulation (PAM-N) systems [3], [4] and passive optical networking (PON) systems based on IM-DD [5], [6]. In addition to discrete reflections among connectors and splicings, optical Rayleigh backscattering places more constraint on bidirectional transmission systems [7], because back-scattered light interferes with the light in the opposite direction.

To address MPI issue in IM-DD systems, proposed solutions include reducing the coherent length of optical carriers [8], constructing a high-pass filter [3], [9] and reconstructing the delayed signal [10]. Another approach is code division multiplexing (CDM) in which using orthogonal code-words to suppress unsynchronized paths whose phase shift are uncertain. CDM¹ has been proved with capability of combating MPI [11] and interferometric noise due to Rayleigh backscattering in bidirectional transmission systems [12]. On the other hand, channel bandwidth limitation in IM-DD system can be alleviated by digital equalization and pulse shaping. When signal is shaped by orthogonal pairs of square root raised cosine (SRRC) waveform, digital orthogonal multiplexing can be realized at the same time. Due to the multiplexing functionality with the absence of optical carrier, such a digital filtering technique is called carrier-less amplitude phase (CAP) modulation [13], [14]. Matching filter (MFs) of CAP performs (de)multiplexing digitally and is complementary to other multiplexing methods like CDM. MFs achieve the correlation peak only when downsampling is precise [13], thus it is expected with good robustness to MPI because the signal with uncertain delays will be suppressed.

In this paper, a hybrid CDM coding and filtering method is utilized to combat MPI and bandwidth limitation in IM-DD system. Combination of CDM and CAP filters is realized by performing upsampling twice, which is essential to simultaneously explore the advantages of both. Numerical simulations have been conducted to evaluate the feasibility of CDM/CAP signaling in mitigating MPI. That is followed by 112 Gb/s transmission experiments over an optical IM-DD link with emulated MPI. We characterize the impact of MPI for both unidirectional and bidirectional systems where the BER performance of CDM/CAP and CDM only are compared. The rest of the paper is organized as following. Section 2 describes the principle of CDM/CAP signaling. Section 3 presents the simulation studies including MPI's effects to optical IM-DD link and performance evaluation with distortions of bandwidth limitation and MPI. Section 4 provides the experimental results over optical IM-DD link with presence of emulated MPI. Unidirectional as well as bidirectional 30-km transmissions are demonstrated and the induced performance penalties are investigated and discussed. Section 5 concludes the paper.

2. Principle of Hybrid Coding and Filtering Technique

There are several codeword types for CDM operation, including m-sequence [15], Gold code [16] and Walsh-Hadamard code [17]. Here we employ Walsh-Hadamard code which is also called Walsh code as the codeword to perform CDM signaling. Walsh code can accommodate a larger number of users for a given codeword length compared to m-sequence and Gold code [18]. For a given code length, the codewords w_i with $1 \leq i \leq M$ are generated by Hadamard matrix, where M is multiplexing channel number in code domain. A code chip of CDM is composed of M samples. For CAP filtering, orthogonal multiplexing can be realized cost-efficiently by using digital filter pairs which in this paper are called shaping filter (SF) at the transmitter (Tx) and matching filter (MF) at the receiver (Rx). SF and MF can be constructed as a pair based on SRRC waveform $h(t)$,

$$h(t) = 4\alpha \frac{\cos((1+\alpha)\pi t/T_s) + \frac{\sin((1-\alpha)\pi t/T_s)}{4\alpha t/T_s}}{\pi \sqrt{T_s}(1 - (4\alpha t/T_s)^2)}, \quad (1)$$

where α is the roll-off factor and T_s is the symbol duration. To realize orthogonal multiplexing, $h(t)$ needs to be multiplied with sinusoidal functions. By adapting the central frequency of sinusoidal functions, the multi-band resolving in frequency domain can be realized. Assuming N bands of CAP filtering, the in-phase and quadrature components are given by F_j^I and F_j^Q in 2) and 3), where

¹Throughout this paper, CDM refers in particular to the electrical CDM.

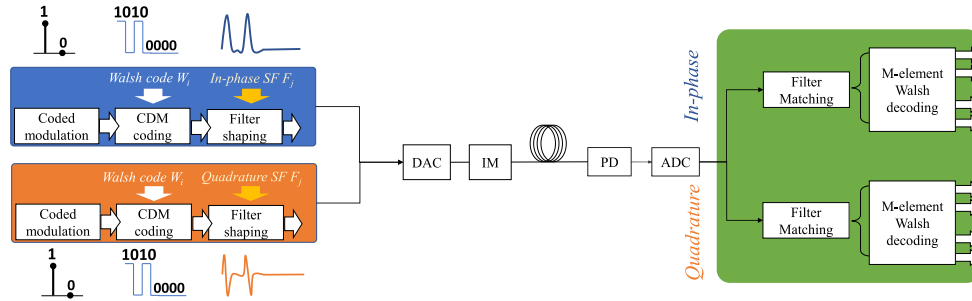


Fig. 1. CDM/CAP signaling over single point to point optical IM-DD link. DAC: digital-to-analogue converter, IM: intensity modulator, PD: photodetector, ADC: analogue-to-digital converter. SF: shaping filter. MF: matching filter.

j denotes the number of frequency bands with $1 \leq j \leq N$.

$$F_j^I = h(t) \cdot \sin((2j - 1)\pi t / T_s), \quad (2)$$

$$F_j^Q = h(t) \cdot \cos((2j - 1)\pi t / T_s). \quad (3)$$

CDM provides the advantages of improved scalability, feasibility of bidirectional transmission and MPI tolerance. On the other hand, CAP filtering provides improved robustness to bandwidth limitation and MPI tolerance as well. As a consequence, the above merits can be simultaneously explored through the implementation of hybrid coding and filtering method. A schematic diagram of the hybrid signaling over IM-DD link is given in Fig. 1. As defined previously, chip length of Walsh codeword is M , and the number of frequency bands of CAP filtering is N . Thus, total number of digital channel is $2M * N$, the factor of '2' is due to the orthogonality of the in-phase and quadrature filters. Coded modulation in the transmitter normally includes channel coding and symbol mapping. After that, CDM coding operates on the symbol level. During this process, the chip rate of CDM signal is $1/M$ times of modulation rate, because upsampling with factor of M is performed before the Kronecker production of symbol and CDM codeword. Then CAP filtering operates waveform shaping after CDM coding, corresponding SFs are given by 2) and 3). Notably, resampling is also required in CAP filtering process. Thus, two rounds of upsampling are mandatory when CDM coding and CAP filtering work together. At the receiver, a photodetector (PD) is used to detect optical signal, and an analogue to digital converter (ADC) samples electrical signal followed by filter matching by MFs and Walsh decoding. Before this work, a joint scheme of CDM and CAP modulation has been proposed [19]. As a following work, we specifically study the feasibility of the hybrid coding and filtering method to combat MPI and bandwidth limitation in IM-DD system. However, the reported 120-Gbps rate in [19] is not precise because the second-round upsampling is not considered,² for the rate loss, even ignoring the FEC overhead (OH). We hereby would like to clarify why two rounds of resampling is mandatory in CDM/CAP system. The first-round upsampling is performed before Walsh coding. The purpose is to map the orthogonal codewords on time-domain sequence. Thus upsampling with factor of M is performed for M -elements CDM coding. Here, Walsh codeword of $[1,1,1,1]$ is chosen to describe CDM/CAP signaling process. Information symbol duration T_R is broadened by the factor of 4 when sampling rate T_s is fixed. The second-round upsampling is performed before waveform shaping by SF. That is because FIR filtering is operated by convolution, that induces overlap among the adjacent points unless FIR filter is unit pulse. If coded sequence is upsampled by the factor of 2, the information symbol duration T_R will be further broadened by factor of 2. On the contrary, if no second-round upsampling is

²As reported in [19], baud rate of DA is 20 G and QAM64 format is employed with 6-bits/symbol spectrum efficiency. Because CDM signaling does not change information rate, the reported rate of 120 Gbps was based on calculation of $20 \times 6 = 120$ Gbps.

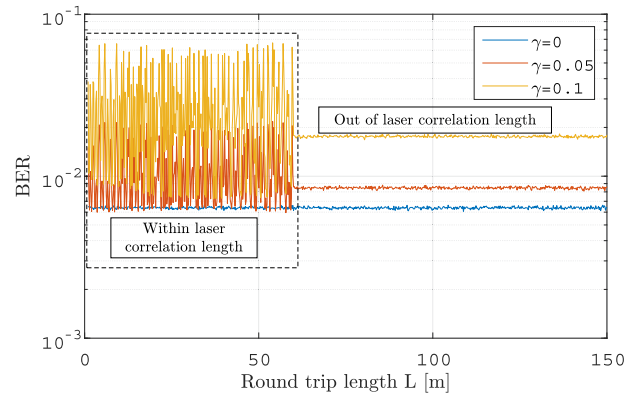


Fig. 2. BER of 112-Gbps PAM4 under different MPI conditions by changing round-trip length L and amplitude ratio γ , with laser linewidth at 5 MHz.

performed, a coded symbol by $[1,1,1,1]$ will overlap among the adjacent symbols, which causes ISI. As for the overlap within a single CDM chip, it induces noise to CDM decoding. Consequently, two rounds of resampling are mandatory for CDM/CAP signaling.

3. Simulation Results

Models developed for optical IM-DD link in this paper are available online [20], including bandwidth channel limitation and MPI modeling, digital implementation of CDM/CAP signaling and performance evaluations as well.

3.1 MPI Model and Its Impacts on Bandwidth-Limited Optical IM-DD Link

There have been several researches on the MPI mechanism, effects and corresponding solutions [21], [22]. A simplified model of MPI was studied [23] and it is based on the approximation that the strongest reflections happen between adjacent connectors and spliced points. It is reasonable because the reflection ratio at each component is much smaller than 1. Throughout this paper, γ represents the amplitude ratio between reflected light and transmitting light. MPI is determined by γ and round-trip delay length L between adjacent reflections. The electric field of an intensity-modulated light $E(t)$ is given by

$$E(t) = \sqrt{A(t)} \cos(w_c t + \phi(t)), \quad (4)$$

where $\sqrt{A(t)}$ is the electrical signal for intensity modulation, w_c is the light angular frequency and $\phi(t)$ is phase. In the case of reflections between adjacent points [24], MPI distortion after square-law detection in the worst case with aligned polarization can be characterized by,

$$P(t) = A(t) + \gamma^2 A(t - t_d) + 2\gamma \sqrt{A(t)} \sqrt{A(t - t_d)} \cos(\phi(t) - \phi(t - t_d)), \quad (5)$$

where $P(t)$ denotes the received power for square-law detection. t_d is the round-trip time between two reflection points. $\phi(t) - \phi(t - t_d)$ term denotes the phase difference between two paths. As a result, MPI results in not only the delayed path (the second term in right-hand side in 5), but also the phase noise dependent distortion (the third term in right-hand side in 5). If time delay t_d is within the range of laser correlation length, $\phi(t) - \phi(t - t_d)$ equals to $w_c t_d$. When t_d exceeds laser correlation length, $\phi(t) - \phi(t - t_d)$ term can be modeled as random phase noise $N_p(t)$ with variance $\sigma_p^2 = 2\pi \Delta v t_d$ where Δv denotes the 3-dB line-width of the carrier [3]. BER values under different round-trip length L are estimated as shown in Fig. 2. Baud rate is set at 56 Gbaud, sampling rate F_s is set at 16 times of baud rate to ensure smooth waveforms for simulation. Laser linewidth is 5 MHz, thus laser correlation length L_c is 60 m. It can be seen from Fig. 2 that when MPI occurs with round

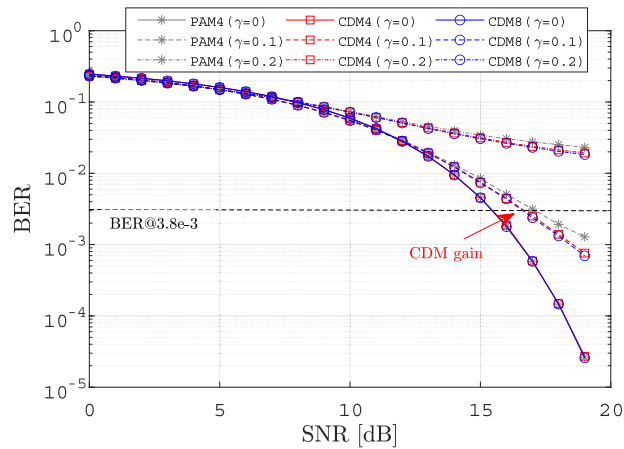


Fig. 3. CDM signaling improvement when MPI distorts with round-trip length of 50 m.

TABLE 1

Benchmarks of SNR Requirement (@ $3.8 \cdot 10^{-3}$ BER) When MPI Distorts With $\gamma = 0.1$

Modulation	CDM8	CDM16	CDM4/CAP2	CDM8/CAP2	CDM4/CAP4
SNR (dB)	15.73	15.69	14.17	14.15	15.7

trip length L smaller than laser's correlation length, BER degraded by MPI fluctuates a lot. That is because within laser's correlation length the phase variance induced by MPI is dependent to relative time delay between two paths. When round trip length L exceeds laser's correlation length (60 m), phase variance can be modeled by Gaussian noise. In that case, BER degraded by MPI becomes smoother as showed in Fig. 2. So one solution to alleviate MPI is to decrease laser coherence [8].

CDM can suppress the asynchronous paths whose time delay is uncertain. Thus, CDM provides a low-cost solution to MPI especially when it occurs within laser correlation length. Fig. 3 shows the performance improvement by CDM to PAM-4 format with round-trip length at 50 m. CDM4 modulation in this paper refers to the signal coded by 4-elements Walsh code word. In the MPI-free case, CDM has the same BER performance with traditional PAM4. When γ is increased to 0.1, CDM can reduce SNR requirement by 0.33 dB to reach BER at 0.0038. It can also be seen from Fig. 3 that there is ignitable difference between CDM4 and CDM8. However in the strong MPI case with $\gamma = 0.2$, even CDM can not recover signal well to reach 0.0038 BER.

3.2 Improvement by CDM/CAP Signaling for MPI-Distorted and Bandwidth-Limited Optical IM/DD Link

Fig. 4 describes the BER performance of CDM/CAP signaling when MPI distorts. The level of MPI is adapted through changing γ . Assisted by CAP filtering, reduced BER is obtained in the MPI-free case. Typically, BER below 10^{-6} can be reached with SNR over 20 dB by CDM4/CAP2 and CDM8/CAP2 signaling. Moreover, CDM4/CAP2 is less sensitive to MPI distortion, as indicated by red curves in Fig. 4(a). As indicated in Fig. 4(b), CDM16 exhibits ignitable improvement than CDM8 with presence of MPI. As for two pairs of CAP filter, the performance of CDM4/CAP4 is worse than CDM/CAP2 as showed in Fig. 4(c). Thus, CDM/CAP2 signaling is preferable to combat MPI distortion in IM-DD link. In order to clarify the performance improvement by CDM/CAP in MPI-distorted IM-DD link, minimum SNR values to reach 7%-OH FEC threshold for different modulations

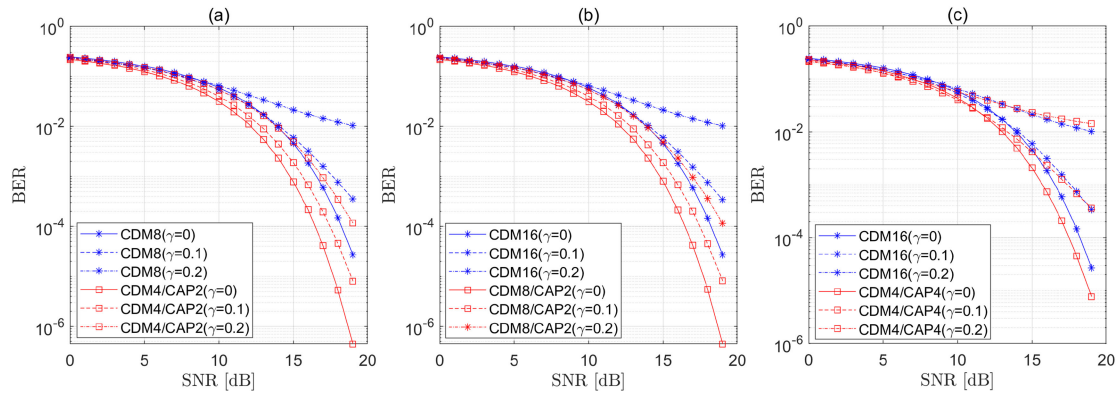


Fig. 4. Simulated BER performance of CDM/CAP in MPI-distorted IM-DD link compared with CDM only method, in the case of (a) 8 digital channels, (b) 16 digital channels with a pair of CAP filter, (c) 16 digital channels with two pairs of CAP filter.

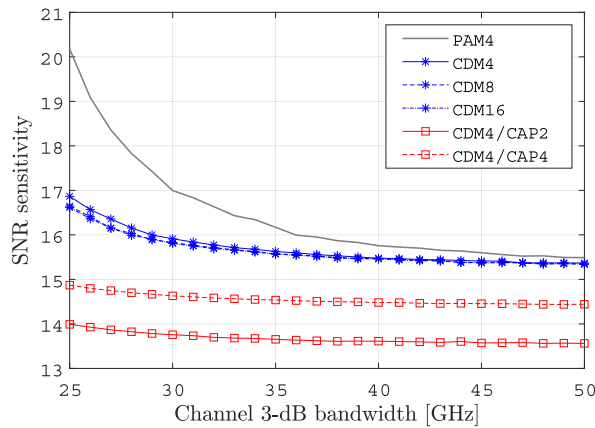


Fig. 5. CDM signaling improvement when MPI distorts with round-trip length of 50 m.

are given in Table 1. It indicates that CDM/CAP2 signaling has 1.5-dB advantage than CDM only method, for combating MPI distortion.

CAP filter can shape signal spectrum, thus CDM/CAP is expected with improved performance for addressing channel bandwidth limitation as well. Here we define SNR sensitivity as the minimum SNR value to reach 7%-OH FEC threshold. Fig. 5 plots SNR sensitivity vs. channel 3-dB bandwidth for different modulations. CDM only method has better bandwidth robustness than traditional PAM4. There is little difference among CDM8 and CDM16. Assisted by CAP filtering, further improved SNR sensitivity can be obtained. Moreover, signaling performance of CDM/CAP exhibits a rather robustness to channel bandwidth, as indicated by the red lines in Fig. 5.

4. Experimental Results

4.1 Unidirectional Transmission With Presence of MPI

Experimental setup of CDM/CAP signaling over optical IM-DD link is shown in Fig. 6. Intensity modulation is realized by modulating a 40-GHz Mach-Zehnder modulator (MZM) using an 8-bit arbitrary waveform generator (AWG). Signal generated by AWG has bandwidth at 30 GHz. Here a Mach-Zehnder interferometer (MZI) is used for emulating MPI. This approach is derived from

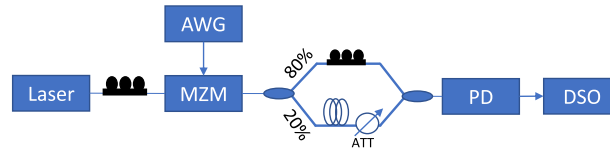


Fig. 6. Experimental setup for optical IM/DD link with emulated MPI distortion.

TABLE 2
Rate Settings for Different Formats in the Experiment

Modulation	CDM8	CDM16	CDM4CAP2	CDM8CAP2
Baud rate	56Gbaud	56Gbaud	84Gbaud	84Gbaud
Upsampling factor in CAP filtering process	1	1	3	3
Bit rate	112Gbps	112Gbps	112Gbps	112Gbps

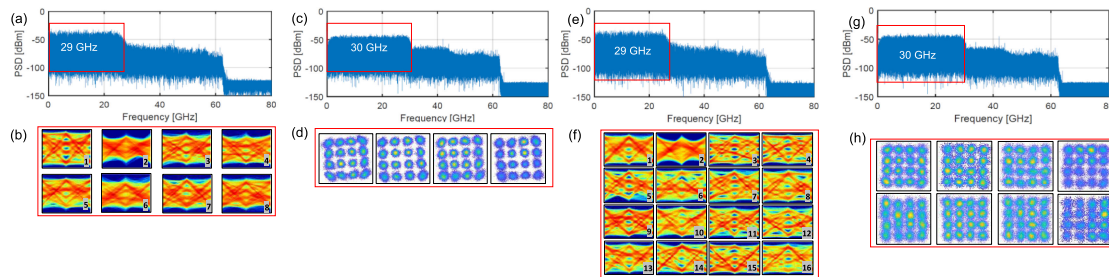


Fig. 7. Received spectra and signal distributions in optical back-to-back case. (a)–(b) 112-Gbps CDM8; (c)–(d) 112-Gbps CDM4/CAP2; (e)–(f) 112-Gbps CDM16; (g)–(h) 112-Gbps CDM8/CAP2.

the MPI model in [23], which is based on that the strongest reflections occurred between adjacent connectors and spliced points. A polarization controller (PC) is used to align the polarization of signal and MPI to simulate worst-case MPI. The other branch injected with 20% power is 1-km SMF. At the receiver, a photo detector (PD) with 30-GHz bandwidth is used for signal detection and the signals are captured by a digital storage oscilloscope (DSO) with 59-GHz bandwidth and 160-GSa/s sampling rate. CDM signals are upsampled at factor of 3 at the second round. Bit rate and baud rate settings for different formats are given as Table 2.

The signal spectra, received signal distributions and eye-diagrams for back-to-back case are shown in Fig. 7. (a) and (c) are the spectra of 112-Gbps CDM8 and CDM4/CAP2 signal respectively. For 112-Gbps CDM8, the second lane coded by $[1, -1, 1, -1, 1, -1, 1, -1]$ and the sixth lane coded by $[1, -1, 1, -1, -1, 1, -1, 1]$ have the worst performance as indicated by eye-diagrams in Fig. 7(b). That is because these two code words locates the corresponding tributaries to higher frequencies, making them more sensitive to bandwidth limitation. CDM4/CAP2 can address this problem with a sharper spectrum edge as showed in Fig. 7(c). The resulted signal distributions become clear as showed in Fig. 7(d). As for 16-lane multiplexing, CDM8/CAP2 has similar spectra to CDM/CAP2, as showed in Fig. 7(g). That is because they have the same shaping filter. The eye-diagrams of CDM16 in Fig. 7(f), shows that the multiplexed tributaries degrades differently. Assisted by CAP, signal distributions over different channel become clear, as showed in Fig. 7(h). In order to alleviate BER degradation due to phase rotation as indicated in Fig. 7(d), we decode the constellation signals to bit stream by finding the nearest labels to every samples.

MPI distortion is emulated by constructing a MZI in Fig. 6. Because the coupling ratio of optical coupler in MZI is 20 : 80, the emulated MPI distortion can be characterized by $\gamma^2 = 0.25$ (γ is

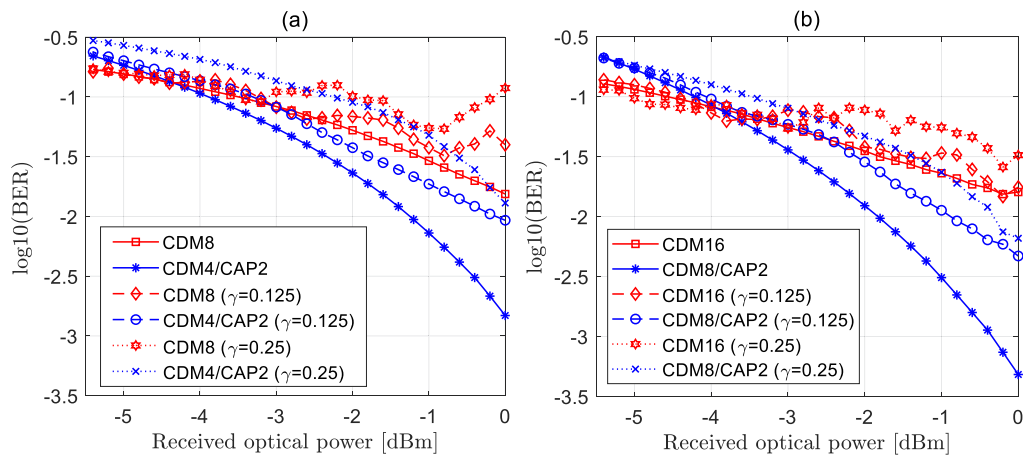


Fig. 8. BER vs. power curves at 112 Gbps when MPI distorts for (a) 8 digital channels case and (b) 16 digital channels case.

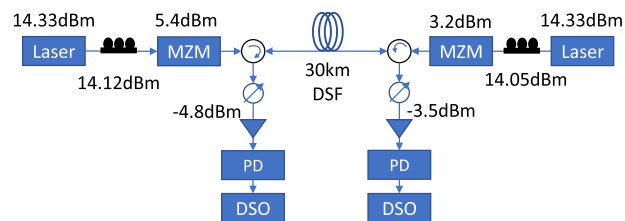


Fig. 9. Experimental setup of bidirectional transmissions.

predefined as the amplitude ratio between reflected and transmitted light). An optical attenuator with fixed attenuation of 3 dB is inserted for obtaining $\gamma^2 = 0.125$. By changing received optical power by a variable optical attenuator (VOA), BER vs. power curve can be used to characterize system performance in the presence of MPI. Firstly, BER vs. power curves for 112-Gbps 8-lane multiplexing are plotted in Fig. 8(a) with different-level MPI distortions. In the MPI-free case, CDM4/CAP2 shows reduced BER at a higher received optical power. Typically for received optical power at 0 dBm, the reduced BER by CDM4/CAP2 goes to $1.5 \cdot 10^{-3}$ that reaches the 7%-OH hard-decision FEC threshold. When power decreases, the BER difference between CDM8 and CDM4/CDM2 becomes smaller because SNR is a dominate issue impeding signaling performance. When MPI distortion is added with $\gamma^2 = 0.125$, the BER curves are plotted as dashed lines in Fig. 8(a). Reduced improvement by CDM4/CAP2 signaling can be observed at a low power value. This is because only sufficient SNR can ensure a good mitigation of MPI. Even though the improvement by CDM/CAP is expected to decrease at low SNR values, it still enables a BER below 10^{-2} at the received optical power of 0 dBm. The performance for 16 digital channels case are shown in Fig. 8(b). In the MPI-free case, reduced BER values can be obtained through CDM8/CAP2 signaling. When MPI distortions are inserted, improvements of CDM8/CAP2 are reduced. With $\gamma^2 = 0.125$, CDM8/CAP2 provides 10 times BER reduction than CDM16 with received optical power of 0 dBm. When $\gamma^2 = 0.25$, CDM16 cannot reach BER of 0.02 while CDM8/CAP2 can reach that target at the received power of 0 dBm.

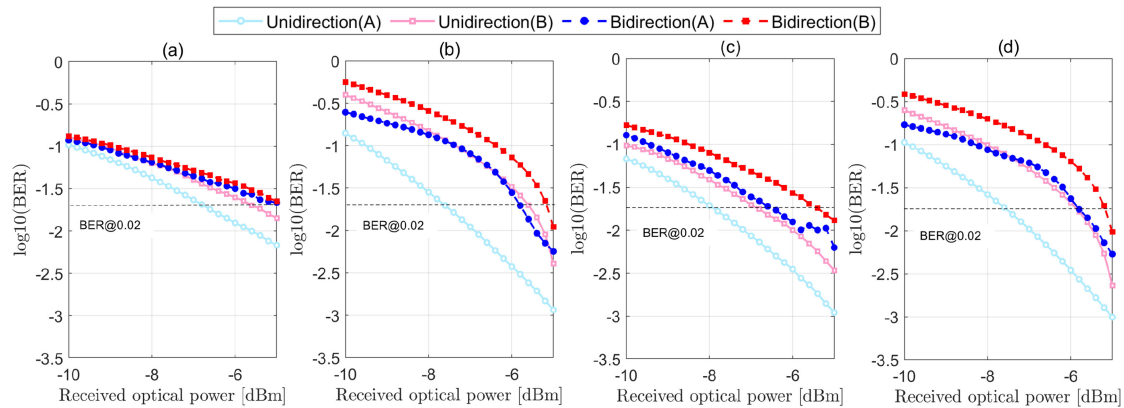


Fig. 10. BER vs. optical power curves for 112-Gbps unidirectional and bidirectional transmission using (a) CDM8, (b) CDM4/CAP2, (c) CDM16, (d) CDM8/CAP2.

4.2 Bidirectional Transmission

Setup for bidirectional transmission is depicted in Fig. 9. To realize bidirectional transmission over a single fiber, two optical circulators are used at both sides. Wavelength of two laser sources in the opposite direction is both at 1550.2 nm. Dispersion-shifted fiber (DSF) is employed for data transmission to enable 30.5-km transmission of IM-DD signals at 1550 nm. Corresponding power values after each component are given in Fig. 9. Because the received optical power is not high enough (-5 dBm after 30-km transmission) to ensure an effective detection of PD (whose sensitivity is 0.4 A/W), an EDFA at the receiver are used to amplify the power to 3 dBm.

Fig. 10 depicts the BER vs. optical power for both unidirectional and bidirectional cases. Received optical power denotes the power value before optical amplification at the receiver. Fig. 10(a) shows the BER performance of CDM8 and (b) shows that of CDM4/CAP2. Two transmissions in opposite directions are denoted by 'A' and 'B' in Fig. 10. In the case of unidirectional transmission, BER performances in two opposite directions are different due to the different channel conditions. For unidirectional signaling of CDM8 in Fig. 10(a), BER can reach below 0.02 with received optical power of -5 dBm. By using CDM4/CAP2 method, BER values of both directions have been improved as indicated by Fig. 10(b). In the unidirectional case, CDM4/CAP2 outperforms CDM8. The improvement is due to the CAP's robustness to channel bandwidth limitations. Although BER is degraded for bidirectional transmissions, CDM4/CAP2 signaling enables BER below 0.02 for both directions with optical power at -5 dBm. Results for 16 digital channels case are given in Fig. 10(c) and (d). CDM16 has better BER performance than CDM8 in both unidirectional and bidirectional cases, as indicated in Fig. 10(c). It indicates that CDM coding with more-elements shows improved performance, when channel has bandwidth limitation and MPI. For CDM16 at 0.02 BER threshold (which meets the least requirement of 20%-OH FEC), power penalties of bidirectional transmission for two opposite directions are 1.35 dB and 1.4 dB respectively at the BER of 0.02, as indicated in Fig. 10(c). For direction 'A,' CDM4/CAP2 signaling outperforms CDM only in both unidirectional and bidirectional cases as Fig. 10(a) and (b) indicate. As for CDM8/CAP2 signaling, BER reduction is not so obvious. Especially for direction 'B,' SNR is not sufficient for BER improvement by CDM8/CAP2. Nevertheless, after bidirectional transmission, the induced power penalties at 0.02 BER threshold are 1.78 dB and 0.65 dB for two directions respectively. The faster BER decreasing slopes indicates that when SNR is sufficient CDM8/CAP2 signaling can offer a better tolerance to interferometric noise, which has been verified by simulations.

5. Conclusion

CDM/CAP signaling is investigated to combat MPI and channel bandwidth limitation in optical IM-DD link. Simulations and experiments over unidirectional and bidirectional link have been conducted to verify the advantages. The results indicate CDM/CAP signaling as a potential solution to interferometric noise for both unidirectional and bidirectional communications.

Acknowledgment

The authors wish to thank the anonymous reviewers for their valuable suggestions.

References

- [1] X. Pang *et al.*, "200 gbps/lane IM/DD technologies for short reach optical interconnects," *J. Lightw. Technol.*, vol. 38, no. 2, pp. 492–503, 2020.
- [2] J. Cheng, C. Xie, Y. Chen, X. Chen, M. Tang, and S. Fu, "Comparison of coherent and IMDD transceivers for intra datacenter optical interconnects," in *Proc. Opt. Fiber Commun. Conf. Exhib.*, 2019, pp. 1–3.
- [3] Y. C. Yang, J. Wen, and Y. Bai, "Mitigation of optical multipath interference impact for directly detected PAMn system," *Opt. Exp.*, vol. 28, no. 25, pp. 38317–38333, 2020.
- [4] C. Fludger, M. Mazzini, T. Kupfer, and M. Traverso, "Experimental measurements of the impact of multi-path interference on PAM signals," in *Proc. Opt. Fiber Commun. Conf.*, 2014, pp. 1–3.
- [5] M. Fujiwara, J.-i. Kani, H. Suzuki, and K. Iwatsuki, "Impact of backreflection on upstream transmission in WDM single-fiber loopback access networks," *J. Lightw. Technol.*, vol. 24, no. 2, pp. 740–746, 2006.
- [6] K. Y. Cho, J. L. Yong, H. Y. Choi, A. Murakami, and C. C. Yun, "Effects of reflection in RSOA-based WDM PON utilizing remodulation technique," *J. Lightw. Technol.*, vol. 27, no. 15, pp. 1286–1295, 2009.
- [7] M. Presi, A. Chiuchiarrelli, R. Proietti, P. Choudhury, G. Contestabile, and E. Ciaramella, "Single feeder bidirectional WDM-PON with enhanced resilience to Rayleigh-backscattering," in *Proc. Opt. Fiber Commun. Conf.*, 2010, pp. 1–3.
- [8] P. J. Urban, A. Koonen, G. Khoe, and H. De Waardt, "Mitigation of reflection-induced crosstalk in a WDM access network," in *Proc. OFC/NFOEC 2008-2008 Conf. Opt. Fiber Communication/National Fiber Optic Engineers Conf.*, 2008, pp. 1–3.
- [9] C. Marki, F. Marki, and S. Esener, "Reduction of interferometric optical crosstalk penalty via DC blocking," *Electron. Lett.*, vol. 43, no. 11, pp. 644–646, 2007.
- [10] M. Xu, Z. Jia, J. Zhang, H. Zhang, and L. A. Campos, "Efficient echo-cancellation algorithms for full duplex coherent optical systems," in *Proc. Opt. Fiber Commun. Conf. Exhib.*, 2020, pp. 1–3.
- [11] G. Gupta, M. Kashima, H. Iwamura, H. Tamai, T. Ushikubo, and T. Kamijoh, "A simple one-system solution COF-PON for metro/access networks," *J. Lightw. Technol.*, vol. 25, no. 1, pp. 193–200, 2007.
- [12] Q. Feng *et al.*, "Colorless long-reach duplex WDM-PON with rayleigh backscattering noise mitigation using orthogonal codes," *J. Lightw. Technol.*, vol. 34, no. 3, pp. 845–853, 2016.
- [13] L. Sun, J. Du, and Z. He, "Multiband three-dimensional carrierless amplitude phase modulation for short reach optical communications," *J. Lightw. Technol.*, vol. 34, no. 13, pp. 3103–3109, 2016.
- [14] J. Wei, D. Cunningham, R. Penty, and I. White, "Study of 100 Gigabit Ethernet using carrierless amplitude/phase modulation and optical OFDM," *J. Lightw. Technol.*, vol. 31, no. 9, pp. 1367–1373, 2013.
- [15] H. Tamai *et al.*, "First demonstration of coexistence of standard gigabit TDM-PON and code division multiplexed PON architectures toward next generation access network," *J. Lightw. Technol.*, vol. 27, no. 3, pp. 292–298, 2009.
- [16] Y. Han, S. Liang, L. Wang, and X. Chen, "Optical receiver sensitivity analysis for electronic code division multiple access over passive optical network," in *Proc. Asia Commun. Photon. Conf. Exhib.*, 2010, pp. 1–8, Paper 79890B.
- [17] W. Huang and M. Nizam, "Coherent optical CDMA (OCDMA) systems used for high-capacity optical fiber networks—system description, OTDMA comparison, and OCDMA/WDMA networking," *J. Lightw. Technol.*, vol. 18, no. 6, pp. 765–778.
- [18] H. Ghafouri-Shiraz and M. M. Karbassian, *Optical CDMA Networks: Principles, Analysis and Applications*, Wiley, 2012.
- [19] K. Kakizaki and S. Sasaki, "120-Gbit/s/pol. λ IM-DD Transmission Over 55-Km SSMF With 10-GHz-Bandwidth Intensity Modulator, Single PD, and a Pair of DAC and ADC With 20 GSa/s," in *Proc. Opt. Fiber Commun. Conf.*, Opt. Soc. America, 2019, pp. Th2A-32.
- [20] [Online]. Available: https://github.com/lin-sunflower/Hybrid_CDM-DFM.git
- [21] P. J. Legg, M. Tur, and I. Andonovic, "Solution paths to limit interferometric noise induced performance degradation in ASK/direct detection lightwave networks," *J. Lightw. Technol.*, vol. 14, no. 9, pp. 1943–1954, 1996.
- [22] J. L. Gimlett and N. K. Cheung, "Effects of phase-to-intensity noise conversion by multiple reflections on gigabit-per-second DFB laser transmission systems," *J. Lightw. Technol.*, vol. 7, no. 6, pp. 888–895, 1989.
- [23] N. Kashima, "Study of multipath interference of passive optical networks using hybrid-Raman amplifiers," *IEICE Commun. Exp.*, vol. 2, no. 6, pp. 263–267, 2013.
- [24] D. A. Fishman, D. G. Duff, and J. A. Nagel, "Measurements and simulation of multipath interference for 1.7-Gb/s lightwave transmission systems using single- and multifrequency lasers," *J. Lightw. Technol.*, vol. 8, no. 6, pp. 894–905, 1990.